3 Simple models of heat pumps.

3.1 Introduction

The idea of constructing miniature versions of engines, motors and pumps has been an interesting one. The earliest theoretical construct of such a device is probably Feynman's ratchet and pawl model discussed in [49]. In this article Feynman uses this simple microscopic model to demonstrate why a Maxwell's demon cannot work. In the same article he also shows how this model can be used to construct a microscopic heat engine and discusses its efficiency. There have been a number of recent detailed studies on the pawl-and-ratchet model and some subtle flaws in Feynman's original arguments have been pointed out [48 – 50, 62, 63, 68, 69]. A different class of ratchet models have also been studied in [70 – 77]. In these models Brownian particles, kept in an asymmetric periodic potential and acted upon by periodic time-dependent forces, are found to exhibit directed motion. A number of variations of this model has been studied [78 – 82]. Among its applications it has been proposed that this could provide a mechanism of transport of motors in biological cells [85].

Ratchet models which work on somewhat different principles are models of quantum pumps which are recently being studied theoretically [84 – 90] and have also been experimentally realized [93, 94]. Since these pumps also work at zero temperature it appears that noise is not an essential feature, which is unlike the case for usual ratchet models. Motivated by the quantum particle pump model, Segal and Nitzan have proposed a model for a heat pump [95]. In this model a molecule with two allowed energy levels interacts with two heat reservoirs kept at different temperatures. The energy level difference is modulated in a periodic way. Thus unlike the other particle pump models here only a single parameter is

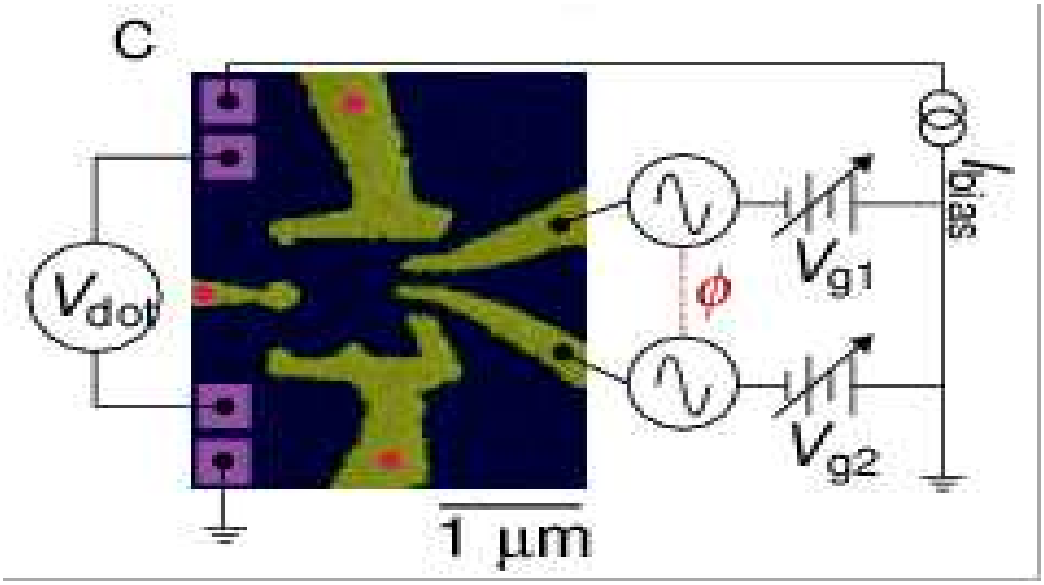

Figure 3.1: Schematic representation of the experimental assembly by Switkes *et al.* [93].

varied. An asymmetry is incorporated by taking reservoirs with different spectral properties and different couplings to the molecule. This seems to lead to the desired pumping of heat from the cold to the hot reservoir.

We will briefly discuss few of the experiments done on the quantum pump. One of the first experiment was by Switkes *et al.* [93], who used the quantum pumping mechanism to produce a $\mathcal{DC}$ current in response to the cyclic deformation of the confining potentials in an open quantum dot. The assembly of the the experiment is as shown in the Fig. (3.1). Three gates marked with red circles control conductance of point-contact leads that connect the dot to electronic reservoirs. In this experiment two coupled quantum dots are separately in contact with particle reservoirs which are at the same chemical potential. One applies $\mathcal{AC}$ gate voltages $V_{g_1} = V_0 \cos(\omega t)$ and $V_{g_2} = V_0 \cos(\omega t + \phi)$ to the two dots respectively. This leads to a net flow of particle current between the two reservoirs whose sign depends on the phase ϕ. This can be seen in Fig. (3.2) where the voltage across the dot which is proportional to the current is plotted as a function of phase difference ϕ. A sinusoidal dependence on ϕ is observed.

The physical picture of such processes can be understood as follows. In Fig. (3.3) we show

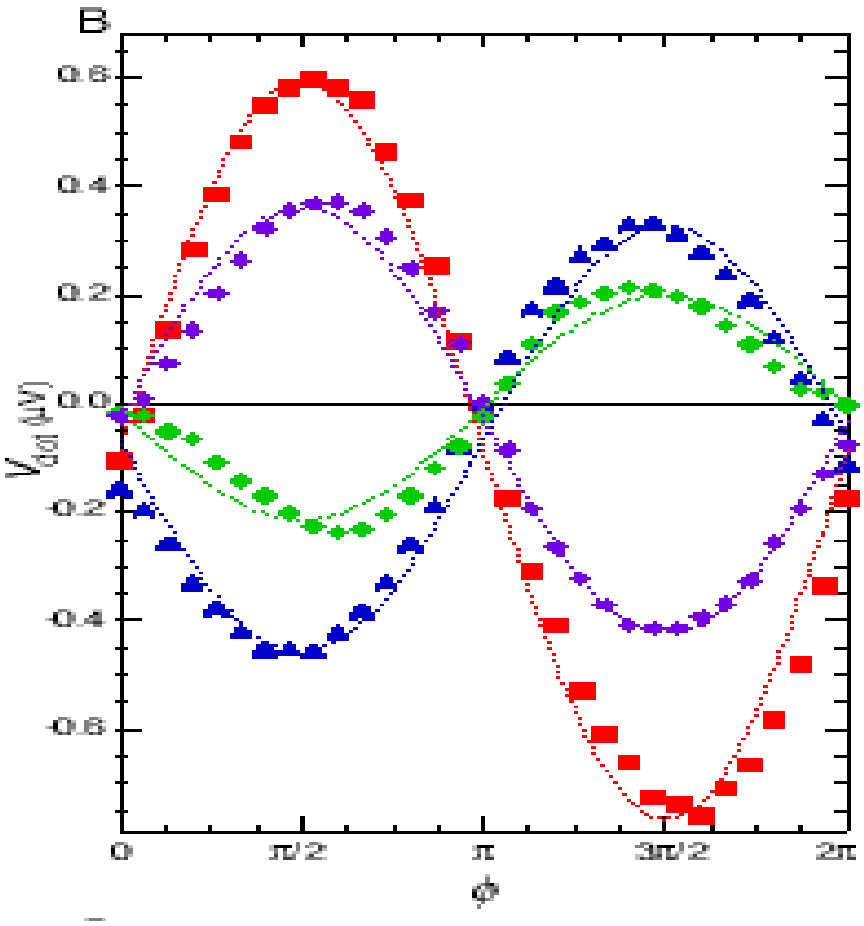

Figure 3.2: Plot of $V_{dot}(\phi)$ as a function of phase ϕ.

a schematic representation of the quantum pump model. Let the phase difference between the voltages be $\phi = \pi/2$. In step (a), a particle from right reservoir is trapped in a potential well $V_2 = -V_0$, in the next step (b), $V_1 = -V_0$ and $V_2 = 0$, so particle goes to the left hand side well. In step (c), $V_2 = V_0$, hence particle cannot go back to the right hand side hence it hops to left reservoir and in step (d), since $V_1 = V_0$, particle cannot hop back. Hence it can be seen that a net charge is transferred from right to left bath, as the potentials vary periodically in time. Also the direction of current depends upon the phase difference ϕ. Another experiment by Leek *et al.* [94] looked charge pumping across a carbon nanotube. The experimental set up is as shown in the Fig. (3.4). A carbon nanotube is attached to the surface of a quartz crystal and connected to reservoirs (source (S) and the drain (D)). A surface acoustic wave

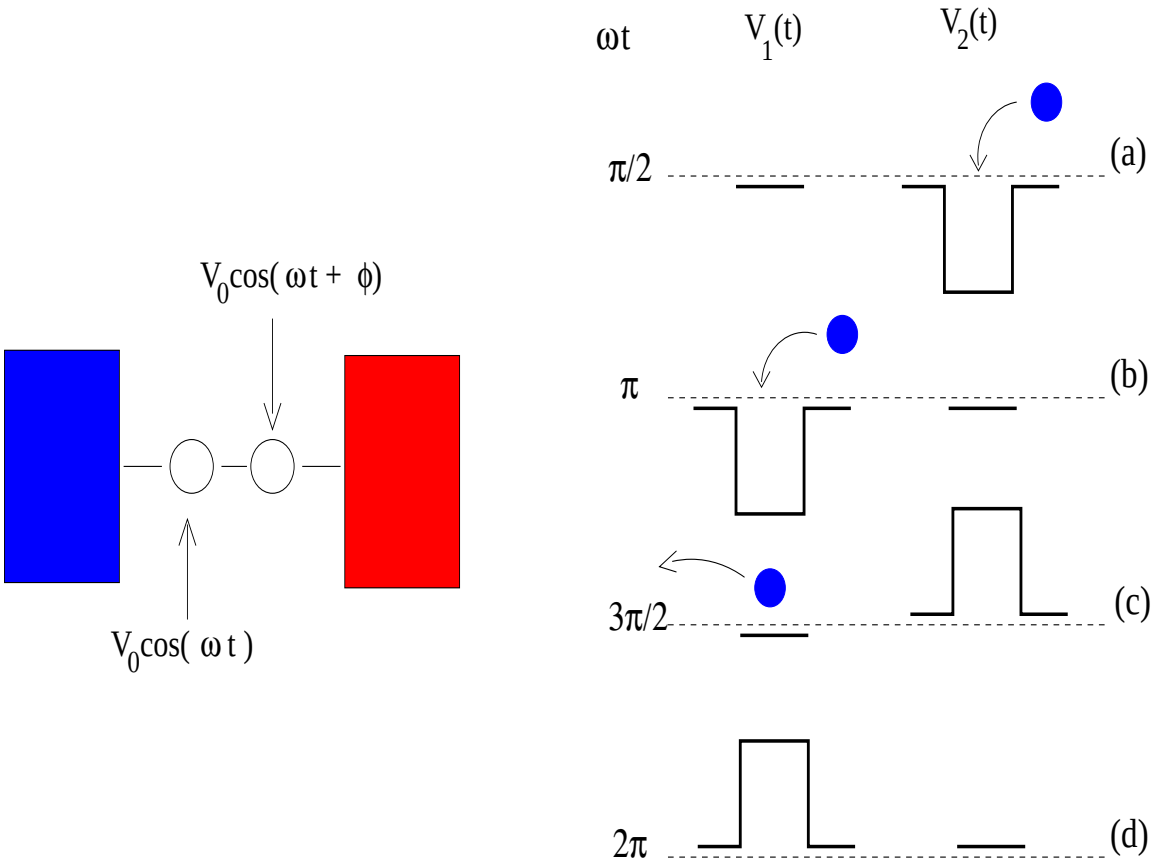

Figure 3.3: Two quantum dots in presence of oscillating voltages. Right hand figures show the two potentials at different times in a cycle. A net charge is transferred in one cycle.

was sent through the quartz crystal, and this produces travelling potential wells inside the nanotubes. It was found that an electron current can be generated across the nanotube as a function of the gate voltage. In this system, the transport of charge resembles the pumping of water by an Archimedean screw (see Fig. (3.5)). In the Archimedean screw, due to the chirality of the pump by rotating the handle water can be pumped to a higher level.

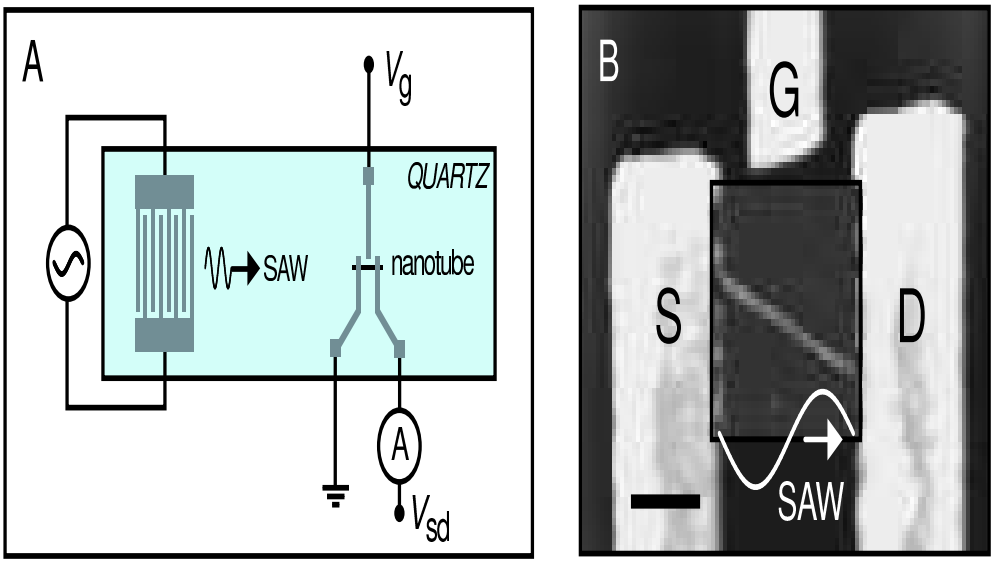

Figure 3.4: Schematic representation of the experimental assembly by Leek *et al.* [94].

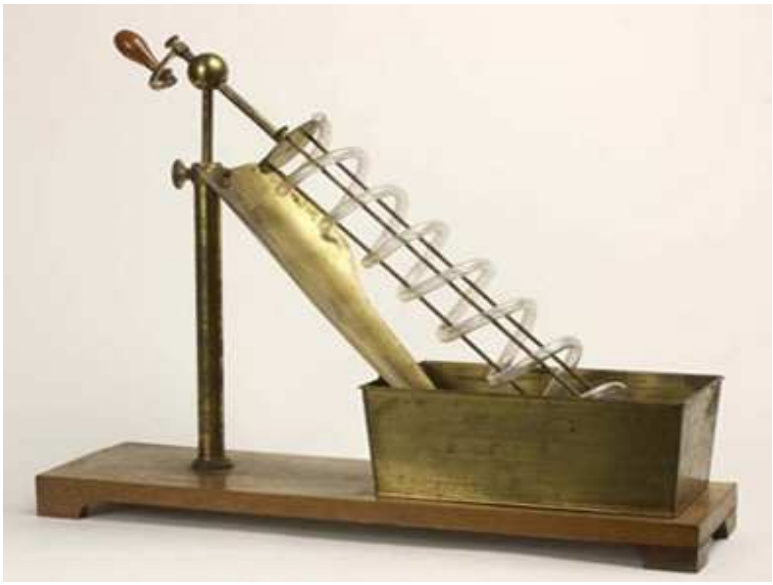

Figure 3.5: Archemedian screw.

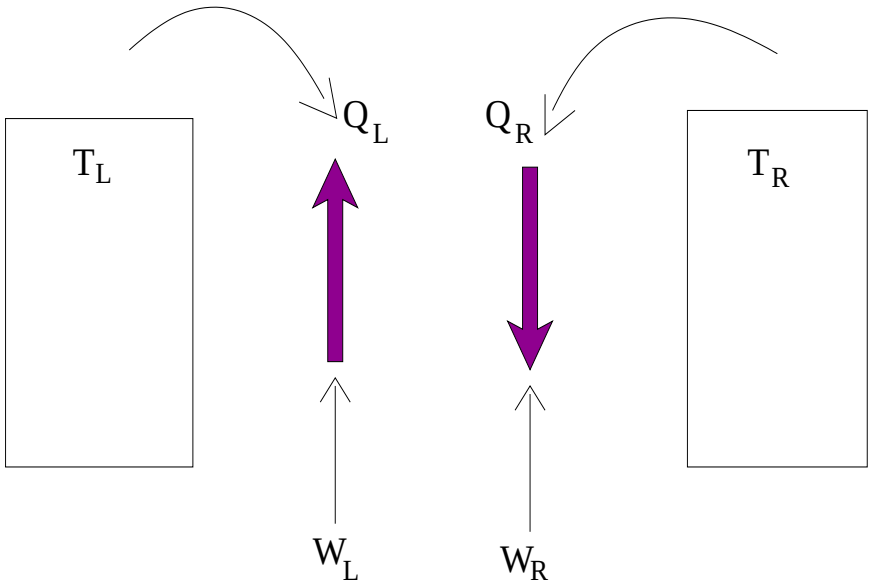

Figure 3.6: System of two Ising spins in contact with two heat baths and are driven by external time dependent magnetic fields.

Motivated by these quantum pump models, we examine classical models of heat pump which have the same basic design. We consider two different models:

1. A spin system consisting of two Ising spins each driven by periodic magnetic fields with a phase difference and connected to two heat reservoirs.

2. An oscillator system of two interacting particles driven by periodic forces with a phase difference and connected to two reservoirs.

In both cases we analyze the possibility of the models to work either as pumps or as engines. Our main result is that the spin system can work both as a pump and as an engine. On the other hand the oscillator model fails to perform either function.

3.2 Spin System

Our first model consists of two Ising spins driven by time-dependent magnetic fields $h_L(t)$ and $h_R(t)$ respectively and each interacting with separate heat reservoirs, see Fig. (3.6). The

Hamiltonian of the system is given by:

$$\mathcal{H} = -J\sigma_1\sigma_2 - h_L(t)\sigma_1 - h_R(t)\sigma_2 \,, \qquad \sigma_{1,2} = \pm 1, \tag{3.1}$$

where J is the interaction energy between the spins. The magnetic fields have the forms $h_L(t) = h_0\cos(\Omega t)$ and $h_R(t) = h_0\cos(\Omega t + \phi)$. The interaction of each spin with the heat baths is modeled by a stochastic dynamics. Here we assume that the time-evolution of the spins is given by Glauber dynamics [96], generalized to the case of two heat baths, with temperatures T_L and T_R. Thus the Glauber spin flip rates for the two spins, arising from the left and right reservoirs are respectively given by:

$$\begin{aligned} r^L_{\sigma_1\sigma_2} &= r\,(1 - \gamma_L\sigma_1\sigma_2)\,(1 - \nu_L\sigma_1) \\ r^R_{\sigma_1\sigma_2} &= r\,(1 - \gamma_R\sigma_1\sigma_2)\,(1 - \nu_R\sigma_2), \end{aligned} \tag{3.2}$$

where

$$\begin{aligned} \gamma_{L,R} &= \tanh(J/k_BT_{L,R}) \\ \nu_{L,R} &= \tanh(h_{L,R}/k_BT_{L,R}) \end{aligned} \tag{3.3}$$

and r is a rate constant. The master equation for evolution of the spin distribution function $\hat{P} = [P(+,+,t), P(-,+,t), P(+,-,t), P(-,-,t)]^T$ is then given by:

$$\frac{\partial\hat{P}}{\partial t} = \mathcal{T}\hat{P}\,, \tag{3.4}$$

where

$$\mathcal{T} = \begin{pmatrix} -r^L_{++} - r^R_{++} & r^L_{-+} & r^R_{+-} & 0 \\ r^L_{++} & -r^L_{-+} - r^R_{-+} & 0 & r^R_{--} \\ r^R_{++} & 0 & -r^L_{+-} - r^R_{+-} & r^L_{--} \\ 0 & r^R_{-+} & r^L_{+-} & -r^L_{--} - r^R_{--} \end{pmatrix}.$$

We define $\dot{Q}_L$, $\dot{Q}_R$ to be the rates (averaged over the probability ensemble) at which heat is absorbed from the left and right baths respectively while $\dot{W}_L$, $\dot{W}_R$ are the rates at which work is done on the left and right spins by the external magnetic field. These can be readily

expressed in terms of the spin distribution function and the various transition rates. Thus we find:

$$\begin{aligned}
\dot{Q}_L &= \sum_{\sigma_1,\sigma_2} P(\sigma_1,\sigma_2,t) r^L_{\sigma_1\sigma_2} \Delta E_1(\sigma_1,\sigma_2) \\
\dot{Q}_R &= \sum_{\sigma_1,\sigma_2} P(\sigma_1,\sigma_2,t) r^R_{\sigma_1\sigma_2} \Delta E_2(\sigma_1,\sigma_2) \\
\dot{W}_L &= -\langle\sigma_1\rangle\, \dot{h}_L = -\dot{h}_L \sum_{\sigma_1,\sigma_2} \sigma_1 P(\sigma_1,\sigma_2,t) \\
\dot{W}_R &= -\langle\sigma_2\rangle\, \dot{h}_R = -\dot{h}_R \sum_{\sigma_1,\sigma_2} \sigma_2 P(\sigma_1,\sigma_2,t)\,,
\end{aligned} \tag{3.5}$$

where

$$\begin{aligned}
\Delta E_1 &= 2\,(J\sigma_1\sigma_2 + h_L\sigma_1) \\
\Delta E_2 &= 2\,(J\sigma_1\sigma_2 + h_R\sigma_2)
\end{aligned} \tag{3.6}$$

are the energy costs in flipping the first and second spin respectively. The average energy of the system is given by

$$U = \langle\mathcal{H}\rangle = \sum_{\sigma_1,\sigma_2} \mathcal{H}(\sigma_1,\sigma_2,t)\, P(\sigma_1,\sigma_2,t). \tag{3.7}$$

Differentiating Eq. (3.7) with respect to time, we get

$$\dot{U} = \sum_{\sigma_1,\sigma_2} \dot{\mathcal{H}}(\sigma_1,\sigma_2,t)\, P(\sigma_1,\sigma_2,t) + \sum_{\sigma_1,\sigma_2} \mathcal{H}(\sigma_1,\sigma_2,t)\, \dot{P}(\sigma_1,\sigma_2,t). \tag{3.8}$$

Differentiating Eq. (3.1) with respect to time and using Eqs. (3.4) and (3.5) in Eq. (3.8), it is easy to verify the energy conservation equation:

$$\dot{U} = \dot{Q}_L + \dot{Q}_R + \dot{W}_L + \dot{W}_R. \tag{3.9}$$

From Floquet's theorem we expect probability distribution $\hat{P}$, at long times to be periodic with time period $\tau = 2\pi/\omega$. We will be interested in the following time averaged rates of

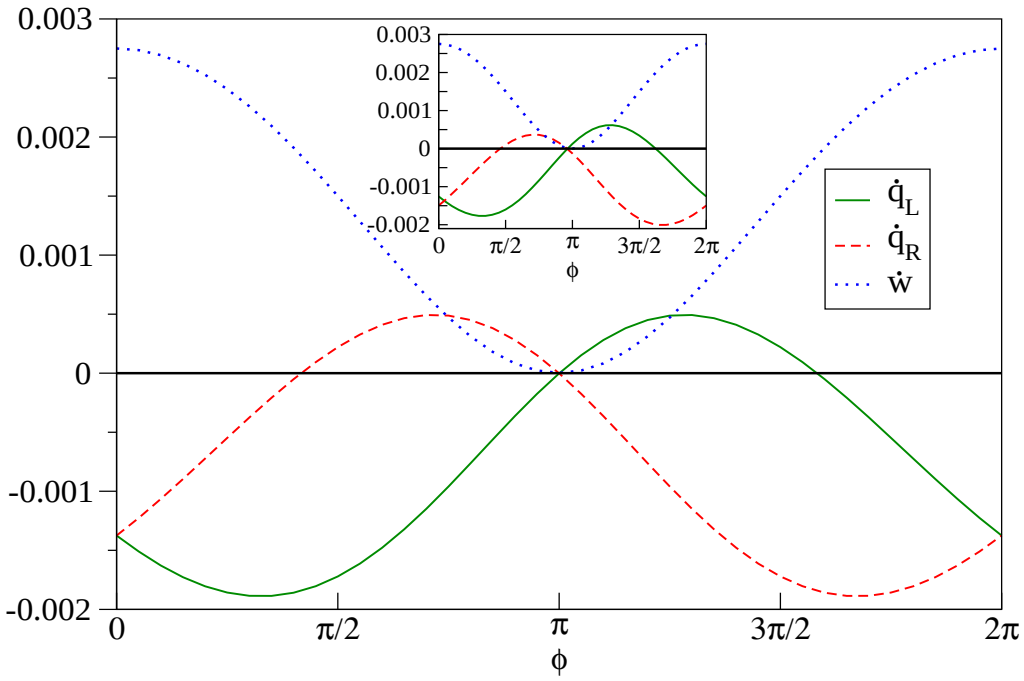

Figure 3.7: Plot of $\dot{q}_L$, $\dot{q}_R$, $\dot{w}$ versus ϕ with both baths at the same temperature. Inset shows the currents for the case where the right bath is slightly colder.

heat exchanges and work done, evaluated in the steady state:

$$\begin{aligned} \dot{q}_{L,R} &= \frac{1}{\tau}\int_0^\tau \dot{Q}_{L,R}\, dt\,, \\ \dot{w}_{L,R} &= \frac{1}{\tau}\int_0^\tau \dot{W}_{L,R}\, dt. \end{aligned} \tag{3.10}$$

We numerically solve the master equation Eq. (3.4) and then evaluate the various steady-state energy exchange rates $\dot{q}_{L,R}$ and $\dot{w}_{L,R}$. In all our numerical calculations we set $r = 0.5$ and $J/k_B = 1$ and all other quantities are measured in these units. In Fig. (3.7) we consider the parameter values $T_L = T_R = 0.5$, $h_0 = 0.25$, $\tau = 225$ and plot $\dot{q}_L, \dot{q}_R$ and $\dot{w} = \dot{w}_L + \dot{w}_R$ as functions of the phase ϕ. It can be seen that, for certain values of the phase, both $\dot{q}_L$ and $\dot{q}_R$ are negative while $\dot{w}$ is positive. Following our sign conventions, this means that all the work from the external driving is getting dissipated into the two baths. More interestingly we find that for certain values of the phase we can get $\dot{q}_L > 0$ and $\dot{q}_R < 0$ which means that there is heat flow *from* the left reservoir *to* the right reservoir. The direction of heat flow can be reversed by changing the phase. From continuity arguments it is clear that this model can also sustain heat flow against a small temperature gradient. Thus the inset of Fig. (3.7) shows

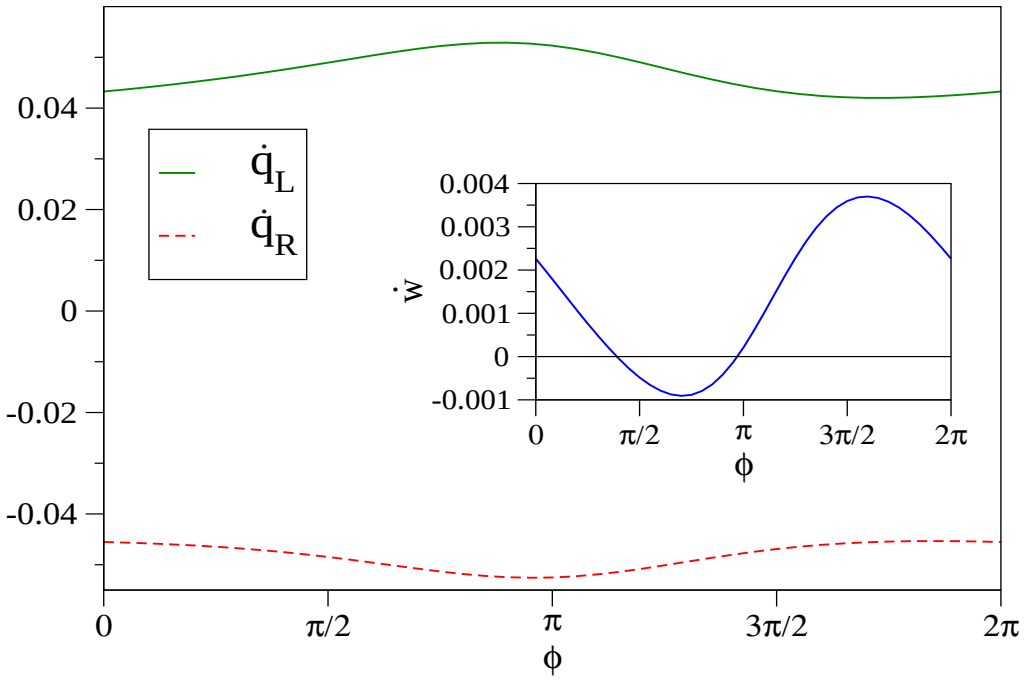

Figure 3.8: Plot of $\dot{q}_L$, $\dot{q}_R$, $\dot{w}$ versus ϕ for parameter values chosen such that the model performs as an engine.

the currents when the right reservoir is kept at a slightly lower temperature $T_R = 0.499$. In the absence of any driving we would get a steady current $\dot{q}_L = -\dot{q}_R = 1.41 \times 10^{-4}$ from the left to right reservoir. In the presence of driving and at a phase value $\phi = 2.2$ we get $\dot{q}_R = 3.674 \times 10^{-4}$, $\dot{q}_L = -1.025 \times 10^{-3}$ which means that heat flows *out* of the cold reservoir. Thus we see that our model can perform as a heat pump or a refrigerator. Similarly we find that the model can also perform like an engine and convert heat to work. This can be seen in Fig. (3.8) where we consider the parameter values $T_L = 1.0, T_R = 0.1$, $h_0 = 0.25$, $\tau = 190$. In this case we find that for certain values of ϕ we can have $\dot{w} < 0$ which means that work is being done on the external force. For typical values of parameters that we have tried we find that the efficiency of the engine is quite low. For example for Fig. (3.8) with $\phi = 0.7\pi$, we find $\eta = |\dot{w}|/\dot{q}_L = 1.75 \times 10^{-2}$.

Finally in Fig. (3.9) we plot the time-dependent energy transfer rates given by Eq. (3.5) for parameter values corresponding to the refrigerator and engine modes of operation. In both cases the initial configuration was chosen with $P(+,+,t=0) = 1$. At long times we

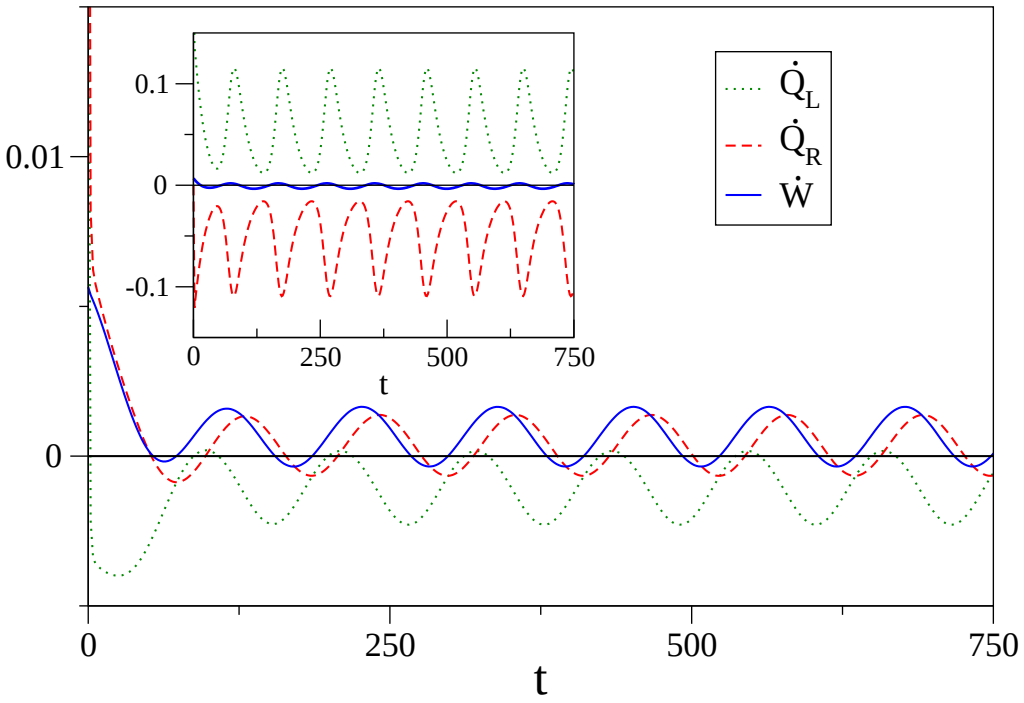

Figure 3.9: Plot of $\dot{Q}_L$, $\dot{Q}_R$, $\dot{W}$ as a function of time for parameters corresponding to pump and engine (inset).

see that all quantities vary periodically with time with the same period τ as the driving force. Fig. (3.9) corresponds to the parameter values $T_L = 0.5$, $T_R = 0.499$, $h_0 = 0.25$, $\tau = 225$ and $\phi = 2.2$ while the inset corresponds to the engine parameters $T_L = 1.0$, $T_R = 0.1$, $h_0 = 0.25$, $\tau = 190$ and $\phi = 2.2$.

3.3 Oscillator System

The second model of our engine consists of two particles which separately interact with two reservoirs kept at different temperatures (see Fig. (3.10)). The particles interact with each other and are also driven by two external periodic forces with a phase difference. We consider the system to be described by the Hamiltonian

$$\mathcal{H} = \frac{p_1^2}{2m} + \frac{p_2^2}{2m} + \frac{1}{2}kx_1^2 + \frac{1}{2}kx_2^2 + \frac{1}{2}k_c(x_1 - x_2)^2 - (f_L(t)\,x_1 + f_R(t)\,x_2). \qquad (3.11)$$

The two particles are acted on by external periodic forces given by $f_L(t) = f_0\cos(\Omega t)$ and $f_R(t) = f_0\cos(\Omega t + \phi)$ respectively, where ϕ is a phase difference. The effect of the heat baths

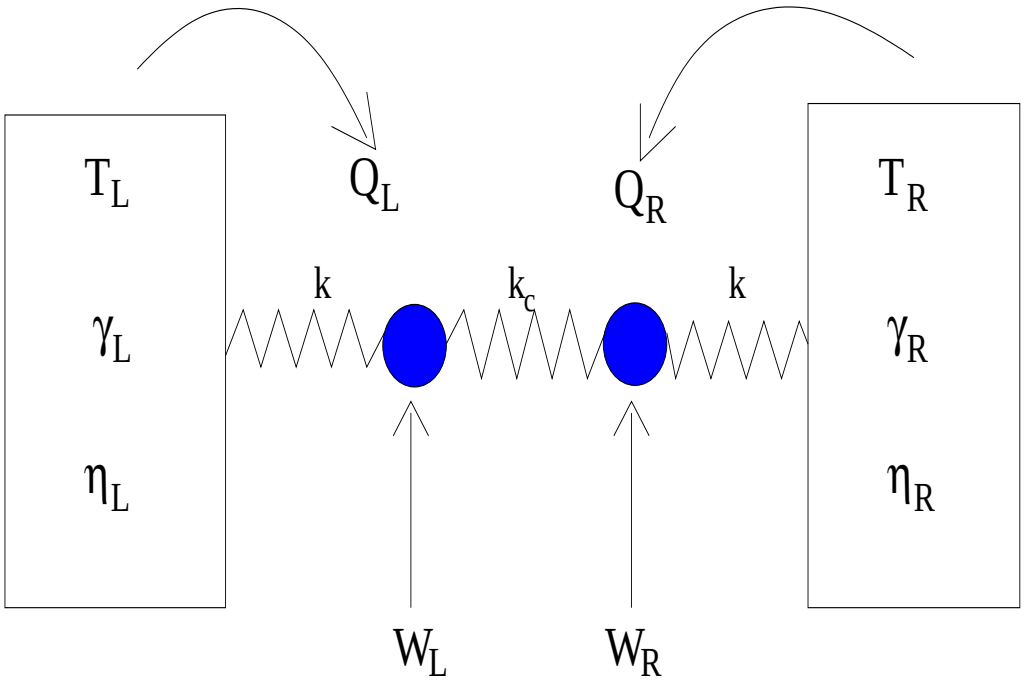

Figure 3.10: System of two Brownian particles in contact with two heat baths and are driven by external time dependent forces.

at temperatures T_L and T_R is modeled by Langevin equations. Thus the equations of motion are

$$\begin{aligned} m\ddot{x}_1 &= -(k+k_c)x_1 + k_c x_2 - \gamma\dot{x}_1 + \eta_L + f_L(t)\,, \\ m\ddot{x}_2 &= -(k+k_c)x_2 + k_c x_1 - \gamma\dot{x}_2 + \eta_R + f_R(t)\,, \end{aligned}$$

where the two noise terms are Gaussian and uncorrelated and satisfy the usual fluctuation-dissipation relations $\langle \eta_{L,R}(t)\eta_{L,R}(t')\rangle = 2k_B T_{L,R}\gamma\delta(t-t')$. Multiplying the two equations above by $\dot{x}_1$ and $\dot{x}_2$ respectively and adding them up we get:

$$\dot{\mathcal{H}} = (-\gamma\dot{x}_1 + \eta_L)\dot{x}_1 + (-\gamma\dot{x}_2 + \eta_R)\dot{x}_2 - \dot{f}_L(t)x_1 - \dot{f}_R(t)x_2, \tag{3.12}$$

which has the obvious interpretation of an energy conservation equation. Averaging over noise we get

$$\dot{U} = \dot{Q}_L + \dot{Q}_R + \dot{W}_L + \dot{W}_R, \tag{3.13}$$

where the various energy exchange rates have the same interpretations as in the previous discussion and are given by,

$$\begin{aligned}
\dot{Q}_L &= \langle(-\gamma\dot{x}_1 + \eta_L)\dot{x}_1\rangle \,, \\
\dot{Q}_R &= \langle(-\gamma\dot{x}_2 + \eta_R)\dot{x}_2\rangle \,, \\
\dot{W}_L &= -\langle \dot{f}_L x_1\rangle \,, \\
\dot{W}_R &= -\langle \dot{f}_R x_2\rangle. \qquad (3.14)
\end{aligned}$$

As before we define the average energy transfer rates in the steady state $\dot{q}_L, \dot{q}_R, \dot{w}_L, \dot{w}_R$. The present model being linear, it is straightforward to exactly compute these as we now show.

We first obtain the steady-state solutions of the equations of motion. We write the equations of motion in the following matrix form:

$$M\dot{X} = -\Phi X - \Gamma\dot{X} + \eta(t) + f(t), \qquad (3.15)$$

where $X = [x_1, x_2]^T$, $\eta = [\eta_L, \eta_R]^T$, $f = [f_0\cos(\Omega t), f_0\cos(\Omega t + \phi)]^T$, M and Γ are diagonal matrices with diagonal elements m and γ respectively and Φ is the force constant matrix. The steady state solution of this equation is:

$$\begin{aligned}
X(t) &= X_N(t) + X_D(t) \,, \\
\text{where } X_N(t) &= \int_{-\infty}^{\infty} d\omega e^{-i\omega t} G(\omega)\tilde{\eta}(\omega) \,, \\
X_D(t) &= Re[G(\Omega)\tilde{f}e^{-i\Omega t}] \,, \\
\text{with } G(\omega) &= [\Phi - \omega^2 M + i\omega\Gamma]^{-1} \,, \qquad (3.16)
\end{aligned}$$

and $\tilde{\eta} = \int_{-\infty}^{\infty} d\omega e^{-i\omega t}\ \eta(t)$, $\tilde{f} = \{1, e^{-i\phi}\}^T$. It is easy to see that the matrix $G(\omega)$ has two independent elements and we denote them as,

$$\begin{aligned}
A(\omega) = G_{11} &= G_{22} = [k + k_c - m\omega^2 - i\gamma\omega]/[(k + k_c - m\omega^2 - i\gamma\omega)^2 - k_c^2] \\
B(\omega) = G_{12} &= G_{21} = k_c/[(k + k_c - m\omega^2 - i\gamma\omega)^2 - k_c^2]. \qquad (3.17)
\end{aligned}$$

Using the above solution in Eq. (3.16), and after some bit of algebraic simplifications, we

obtain the following results:

$$\begin{aligned}
\dot{q}_L &= -\frac{f_0^2\Omega}{2}\,[\,A_I(\Omega) + B_I(\Omega)\cos(\phi) + D(\Omega)\sin(\phi)\,] + \frac{k_B\gamma k_c^2(T_L - T_R)}{2(mk_c^2 + (k+k_c)\gamma^2)}\,, \\
\dot{q}_R &= -\frac{f_0^2\Omega}{2}\,[\,A_I(\Omega) + B_I(\Omega)\cos(\phi) - D(\Omega)\sin(\phi)\,] + \frac{k_B\gamma k_c^2(T_R - T_L)}{2(mk_c^2 + (k+k_c)\gamma^2)}\,, \\
\dot{w}_L &= \frac{f_0^2\Omega}{2}\,[\,A_I(\Omega) + B_I(\Omega)\cos(\phi) - B_R(\Omega)\sin(\phi)\,]\,, \\
\dot{w}_R &= \frac{f_0^2\Omega}{2}\,[\,A_I(\Omega) + B_I(\Omega)\cos(\phi) + B_R(\Omega)\sin(\phi)\,], \qquad (3.18)
\end{aligned}$$

where $A_R,\ A_I,\ B_R,\ B_I$ are the real and imaginary parts of A and B respectively and $D(\Omega) = 2\gamma^2\Omega^2 k_c/Z(\Omega)$ where $Z(\Omega) = |(k+k_c-m\Omega^2-i\gamma\Omega)^2 - k_c^2|^2$. From the expressions in Eq. (3.18) it is clear that the heat transfer rates can be separated into deterministic parts (depending on the driving strength f_0) and noise parts (dependent on temperature of the two reservoirs). The work terms are temperature independent. We now note that the deterministic parts of $\dot{q}_L$ and $\dot{q}_R$, are both negative. This can be shown by using the facts that $A_I \geq 0$ and $A_I^2 - B_I^2 - D^2 = \gamma^2\Omega^2[(k + k_c - m\Omega^2)^2 + \gamma^2\Omega^2 - k_c^2]^2/Z^2 \geq 0$. This means that for $T_L > T_R$, we always get $\dot{q}_R < 0$ and hence we can never have heat transfer from the cold to the hot reservoir. Thus this *cannot* work as a heat pump. Also we note that while $\dot{w}_L$ and $\dot{w}_R$ can individually be negative, the total work done $\dot{w}_L + \dot{w}_R$ is always positive. This means that this model *cannot* work as an engine either. These conclusions remain unchanged even if we define work as $\dot{W}_L = \langle f_L\dot{x}_1\rangle$, $\dot{W}_R = \langle f_R\dot{x}_2\rangle$. In Fig. (3.11) we plot the dependence of the rates of heat transfer and work done in the system on the phase difference ϕ. The figures correspond to the parameter values $k = 2,\ k_c = 3,\ m = 1,\ f_0 = 1,\ \gamma = 1$ and $T_L = T_R = T$. The plots are independent of the temperature T. Note that the only effect of the driving is to pump in energy which is asymmetrically distributed between the two reservoirs. The asymmetric energy transfer into the baths is an interesting effect considering that there is no inbuilt directional asymmetry in the system.

In this model the heat baths and the external driving seem to act independently on the system. It is clear that the linearity of the model leads to this separability of the effects of the driving and noise forces and this could be the reason that the model is not able to function as a

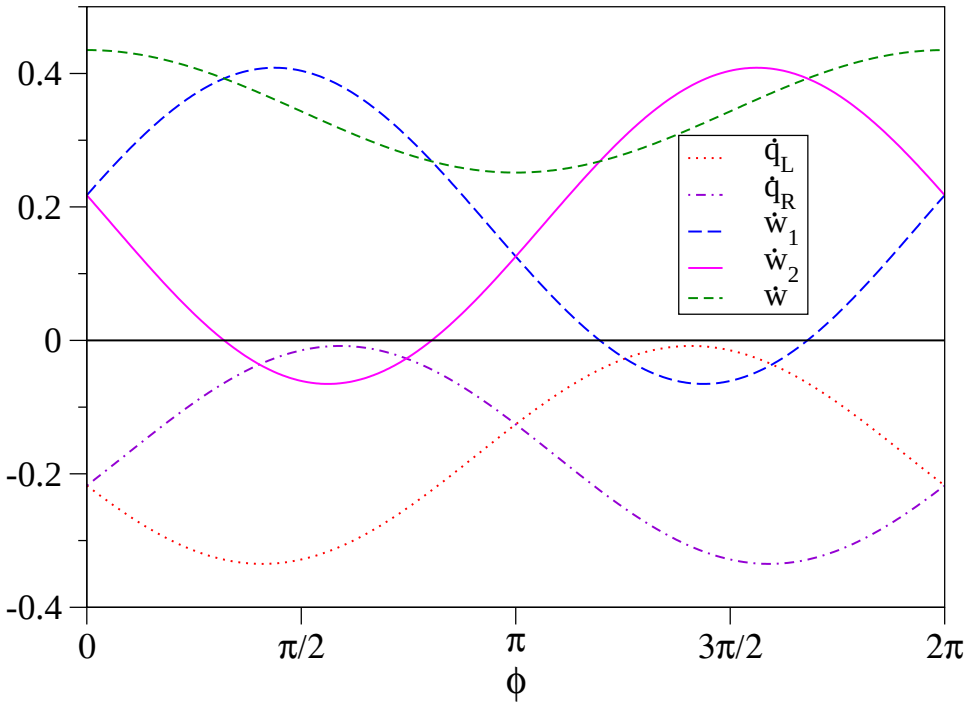

Figure 3.11: Plots of heat transfer and work done as a function of phase difference ϕ in the two particle model. Here $\Omega = 2\pi/3$.

heat pump. Hence it is important to consider the effect of non-linearity. We have numerically studied the effect of including a nonlinear part of the form $\alpha[x_1^4 + x_2^4 + (x_1 - x_2)^4]/4$, in the oscillator Hamiltonian. From simulations with a large range of parameter values we find that the basic conclusions remain unchanged and the model does not work either as a pump or as an engine. In Fig. (3.12) we show some typical results and see that here also even though two works w_L and w_R become negative, still total work done is always positive. Similarly heat transferred is always negative. In Fig. (3.13) we plot the total work done on the system, due to non-linearity we find that this work done now depends on the temperature unlike the linear model.

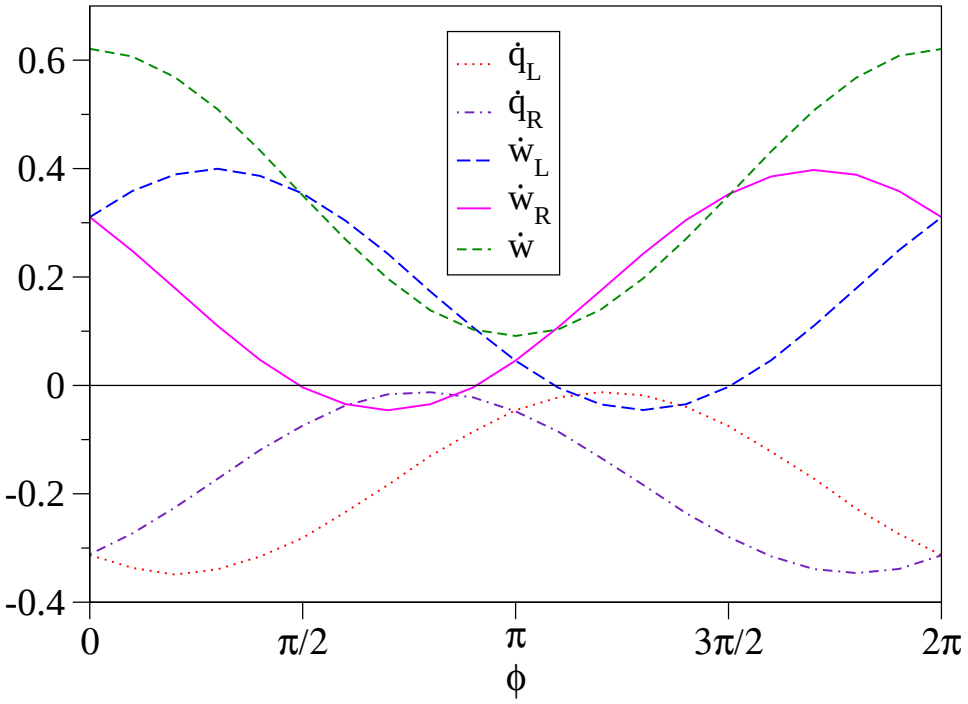

Figure 3.12: Plots of heat transfer and work done as a function of phase difference ϕ in the two particle model with non-linearity. Here $\Omega = 2\pi/3$ and other parameters same as in Fig. (3.11).

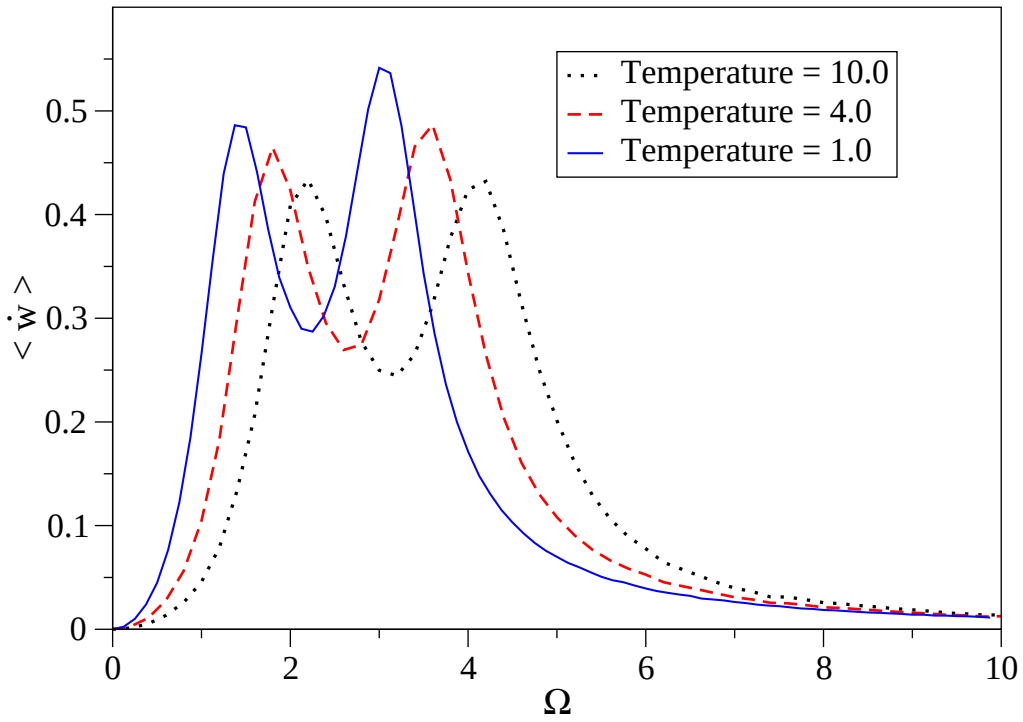

Figure 3.13: Plots of total work done as a function of frequency Ω in the two particle model with non-linearity. Here $\phi = \pi/2$ and other parameters same as in Fig. (3.11).

3.4 Conclusions

In conclusion, we have studied two models which have the same ingredients as those on which recent models of quantum pumps have been constructed. We find that the first model performs as a heat pump to transfer heat from a cold to a hot reservoir. Thus pumping is not an essentially quantum-mechanical phenomena. Also our model performs as an engine to do work on the driving force. It is useful to compare our model with the other well-studied microscopic model of a engine, namely the Feynman ratchet and pawl. Recent detailed studies have shown that this model can function both as an engine and as a refrigerator [53, 54]. One difference of this model from ours is that there is no periodic external driving. However this also means that in order for the model to work in a cyclic way, at least one of the degrees of freedom has to be a periodic (or angular) variable. This may not always be a desirable feature in realistic models. Surprisingly our second model, though apparently built on the same principles, fails to perform either as a pump or as an engine. We have also tried the double well potential of type, $-\frac{1}{2}\,kx_1^2 + \frac{1}{4}\,\alpha x_1^4 - \frac{1}{2}\,kx_2^2 + \frac{1}{4}\,\alpha x_2^4$, which resembles the two levels (in spin case). Though we have tried large range of parameter values, still it is not clear as to what are the necessary conditions for the pump model to work.

The important difference between microscopic models of heat engines, such as those studied here, and usual thermodynamic heat engines is that here the effects of thermal fluctuations are important. A second difference is that here the system is simultaneously in contact with both the cold and hot baths. The understanding of these microscopic models requires the use of non-equilibrium statistical mechanics and there are currently no general principles as in classical thermodynamics. It is clear that further studies are necessary to understand the pumping mechanism in simple models of molecular pumps and this can perhaps lead to more realistic and practical models of molecular pumps and engines.